

Bone regeneration through controlled release of bone morphogenetic protein-2 from 3-D tissue engineered nano-scaffold

Hossein Hosseinkhani ^{a,*}, Mohsen Hosseinkhani ^b, Ali Khademhosseini ^{c,d}, Hisatoshi Kobayashi ^{e,f}

^a International Center for Young Scientists (ICYS), National Institute for Materials Science (NIMS), Tsukuba, Ibaraki 305-0044, Japan

^b Department of Cardiovascular Medicine, Graduate School of Medicine, Kyoto University Hospital, Kyoto 606-8507, Japan

^c Harvard-MIT Division of Health Sciences and Technology, Massachusetts Institute of Technology (MIT), Cambridge, MA, 02139, USA

^d Center for Biomedical Engineering, Department of Medicine, Brigham and Women's Hospital, Harvard Medical School, Cambridge, MA, 02139, USA

^e Biomaterials Center, National Institute for Materials Science (NIMS), Tsukuba, Ibaraki 305-0044, Japan

^f Institute of Biomaterials and Bioengineering, Tokyo Medical and Dental University, Tokyo 113-8549, Japan

Received 13 September 2006; accepted 16 November 2006

Available online 28 November 2006

Abstract

The objective of the present study was to enhance ectopic bone formation through the controlled release of bone morphogenetic protein-2 (BMP-2) from an injectable three dimensional (3-D) tissue engineered nano-scaffold. We demonstrate that a 3-D scaffold can be formed by mixing of peptide-amphiphile (PA) aqueous solution with BMP-2 suspension. A 3-D network of nanofibers was formed by mixing BMP-2 suspensions with dilute aqueous solutions of PA. Scanning electron microscopy (SEM) observation revealed the formation of fibrous assemblies with an extremely high aspect ratio and high surface areas. *In vivo* release profile of BMP-2 from 3-D network of nanofibers was investigated. In addition, ectopic bone formation induced by the released BMP-2 was assessed in a rat model using histological and biochemical examinations. It was demonstrated that the injection of an aqueous solution of PA together with BMP-2 into the back subcutis of rats, resulted in the formation of a transparent 3-D hydrogel at the injected site and induced significant homogeneous ectopic bone formation around the injected site, in marked contrast to BMP-2 injection alone or PA injection alone. The combination of BMP-2-induced bone formation is a promising procedure to improve tissue regeneration.

© 2006 Elsevier B.V. All rights reserved.

Keywords: Nano-scaffold; Peptide amphiphile; Nanofibers; Self-assembly; Bone regeneration

1. Introduction

It has been reported that bone morphogenetic proteins (BMPs), transforming growth factor- β (TGF- β), and basic fibroblast growth factor (bFGF) can induce bone formation in both ectopic and orthotopic sites *in vivo* [1–6]. BMPs belong to the transforming growth factor- β superfamily and play an important role in osteogenesis and bone metabolism [7,8]. Among them, BMP-2 has a very strong osteoinductive activity. Since recombinant human BMP-2 (rhBMP-2) has become available, many animal studies on the induction of bone formation by implantation of rhBMP-2 using various carriers have been performed [9–11]. However, the use of BMP alone requires large amounts of protein because of its short half-life.

Furthermore, the response to BMPs varies between animal species and primates need larger amounts of BMP (up to milligram quantities) than rodents. To overcome these problems and to reduce the amounts of BMP required, developments in new types of scaffold and combined treatments with other reagents which can enhance bone regeneration have been examined. Some studies have demonstrated that some growth factors, such as bFGF, BMP, and TGF, exhibited their expected biological activities *in vivo* when being combined with various carrier matrices [12–14].

It has been reported that structural proteins fiber such as collagen fibers and elastin fibers have diameters ranging from several ten to several hundred nanometers [15]. It has been shown that three dimensional nano-structure could be fabricated through self-assembly of natural or synthetic macromolecules [16]. Hartgerink et al. reported that when dilute aqueous solutions of peptide amphiphile was mixed with cell suspensions in media,

* Corresponding author. Tel.: +81 29 851 3354; fax: +81 29 860 4706.

E-mail address: hossein.hosseinkhani@nims.go.jp (H. Hosseinkhani).

nanoscaled fibers were formed through self-assembly process [16]. Nanoscaled fibers produced by self-assembly of peptide amphiphile may be a promising approach in designing the next generation of biomaterials for drug delivery and tissue engineering.

In the present study, we hypothesized that self-assembly hydrogels comprising of PA and BMP-2 can be used to fabricate tissue engineering scaffolds to induce ectopic bone formation. To test this hypothesis, 3-D networks of self-assembled PA nanofibers were fabricated by mixing BMP-2 suspension with aqueous solution of PA as an injectable carrier for controlled release of growth factors. We demonstrate the feasibility of this approach to induce ectopic bone formation by showing that BMP-2 release from the 3-D networks of nanofibers enhances ectopic bone formation.

2. Materials and methods

Amino acid derivatives, derivatized resins, were purchased from Sowa Trading Co., Inc., Tokyo, Japan. Human recombinant BMP-2 was obtained from Yamanouchi Pharmaceutical Co., Japan. ^{125}I -Bolton–Hunter Reagent (NEX-120H, 147 MBq/ml in anhydrous benzene) was purchased from NEN Research Products, DuPont, Wilmington, DE. BMP-2 solutions at concentrations of 0.02, 0.04, 0.1, 0.2, 1, and 2 $\mu\text{g}/\mu\text{l}$ were made by using phosphate-buffered saline solution (PBS, pH 7.4) as diluent solution. Other chemicals were purchased from Wako Pure Chemical Industries, Ltd., Osaka, Japan and used as obtained.

2.1. Synthesis of the PA

The PA was prepared on a 0.5-mmol scale by using standard fluorenylmethoxycarbonyl chemistry (F-moc) [17] on a fully automated peptide synthesizer (Peptide Synthesizer Model 90, Advanced ChemTech, Inc., KY, USA). Briefly, 1 equivalent of fluorenylmethoxycarbonyl-Asp-Wang resin was reacted with 5 equivalents of fluorenylmethoxycarbonyl-Gly-OH, 5 equivalents of fluorenylmethoxycarbonyl-Arg(PMC)-OH, 5 equivalents of fluorenylmethoxycarbonyl-Glu(OBt)-OH, 15 equivalents of fluorenylmethoxycarbonyl-Gly-OH, and 20 equivalents of fluorenylmethoxycarbonyl-Ala-OH·H₂O in *N*-methyl-2-pyrrolidone. Deprotection was performed with 25% piperidine/DMF. Couplings were achieved using *N,N*-Diisopropylcarbodiimide (DIPCI)/HOBt in molar ratio of 1:1. Finally, the N terminus was reacted with a fatty acid containing 16 carbon atoms. Cleavage (peptide removal from resin) and the removal of side chain protection groups was performed using 95% trifluoroacetic acid (TFA) with 5% water for 2 h at room temperature. PA obtained was further purified by using high performance liquid chromatography (HPLC, Model LC-6AD, Shimadzu Co., Kyoto, Japan) in a column of Intersil PREP ODS (20 mm × 250 mm) with an eluent of 0.1% TFA/H₂O and CH₃CN at flow rate of 10 ml/min. PA was characterized by matrix-assisted laser desorption ionization-time-of-flight mass spectroscopy (MALDI-TOF MS, Model Biflex III, Bruker Daltonics Inc., USA) and was found to have the expected molecular weight.

2.2. Formation of 3-D network of self-assembled PA nanofibers

3-D network of self-assembled PA nanofibers was formed by first mixing phosphate-buffered saline solution (PBS, pH 7.4) containing 0.02, 0.04, 0.1, 0.2, 1, and 2 $\mu\text{g}/\mu\text{l}$ of BMP-2. Subsequently, a transparent gel-like solid was formed by mixing of BMP-2 solution at concentration of 0.2 $\mu\text{g}/\mu\text{l}$ or higher with 1 wt.% PA aqueous (10 mg/ml) solution in a 1:1 volume ratio.

2.3. Morphological observation

The morphology of self-assembled PA nanofibers was observed with a scanning electron microscope (SEM, S-2380N; Hitachi, Tokyo, Japan). The samples were prepared by network dehydration and critical point drying of samples caged in a metal grid to prevent network collapse. The dried sample was coated with gold on an ion sputterer (E-1010; Hitachi) at 50 mTorr and 5 mA for 30 s and viewed by SEM at a voltage of 15 kV.

2.4. Estimation of *in vivo* degradation of self-assembled PA nanofibers incorporating BMP-2

In vivo degradation of self-assembled PA nanofibers was evaluated in terms of the radioactivity loss of ^{125}I -labeled PA incorporating BMP-2. PA was radioiodinated by the use of ^{125}I -Bolton–Hunter reagent as reported previously for other materials [18]. To introduce ^{125}I residues into amino groups of PA, 30 μl of aqueous ^{125}I -Bolton–Hunter solution was incorporated into 100 mg of PA at 4 °C for 3 h. The radioiodinated PA were rinsed with double distilled water (DDW) by exchanging it periodically at 4 °C for 4 days to exclude non-coupled, free ^{125}I -labeled reagent from ^{125}I -labeled PA. To estimate the *in vivo* degradation of self-assembled PA nanofibers incorporating BMP-2, 50 μl of ^{125}I -labeled PA aqueous solution and 50 μl of BMP-2 solution (at concentration of 0.2 $\mu\text{g}/\mu\text{l}$) were carefully injected separately at the same time into the back subcutis of Fischer male rats, age 6 weeks (Shimizu Laboratory Supplies Co., Ltd. Kyoto, Japan). At 1, 3, 7, 10, 14, 21, and 28 days after injection, the radioactivity of the skin around the injected site (3 × 5 cm²) was measured on a gamma counter (ARC-301B, Aloka Co., Ltd, Tokyo, Japan) to evaluate the remaining radioactivity of tissue around the injected site. Six rats were sacrificed at each time point for *in vivo* evaluation unless otherwise mentioned.

2.5. Estimation of *in vivo* BMP-2 release from self-assembled PA nanofibers

In vivo BMP-2 release assay was evaluated in terms of the radioactivity loss of ^{125}I -labeled BMP-2. The radiolabeling of BMP-2 was performed according to the method of Greenwood et al. [19] and as reported previously for other growth factors [18]. Briefly, 4 μl of Na ^{125}I solution was mixed with 40 μl of 1 mg/ml BMP-2 solution containing 5 mM glutamic acid, 2.5 wt.% glycine, 0.5 wt.% sucrose, and 0.01 wt.% Tween 80 (pH 4.5) in the presence of 0.2 mg/ml of chloramine-T

potassium phosphate-buffered solution (0.5 M, pH 7.5). To stop radioiodination, 100 μl of phosphate-buffered saline solution (PBS, pH 7.5) containing 0.4 mg of sodium metabisulfate was added to the reaction solution. To estimate the *in vivo* BMP-2 release, 50 μl of PA aqueous solution and 50 μl of ^{125}I -labeled BMP-2 were carefully injected separately at the same time into the back subcutis of Fischer male rats, age 6 weeks. As a control, 100 μl of ^{125}I -labeled BMP-2 was injected into the back subcutis of rats. The dose of ^{125}I -labeled BMP-2 was 10 μg (0.2 $\mu\text{g}/\mu\text{l}$) for both cases. At different time intervals, the rat skin including the injected site was removed to evaluate the remaining radioactivity of tissue around the injected site.

3. Animal experiments

All procedures were performed in accordance to specifications of Guideline for Animal Experiments of National Institute for Materials Science, Japan. Fischer male rats, age 6 weeks (Shimizu Laboratory Supplies Co., Ltd. Kyoto, Japan) were anesthetized by intraperitoneal injection (3.0 mg/100 g body weight) of chloral hydrate (Wako Pure Chemical Industries, Ltd., Osaka, Japan) shortly after superficially induced anesthesia by ether inhalation. Rats were divided into 3 groups. Group I, control group ($n=6$), 100 μl of PA aqueous solution was injected into the back subcutis of rats. In group II ($n=24$), 100 μl of BMP-2 solutions (at concentrations of 0.02, 0.04, 0.1, 0.2, 1, and 2 $\mu\text{g}/\mu\text{l}$) were injected into the back subcutis of rats ($n=6$ for each concentration). Group III ($n=24$), 50 μl of PA aqueous solution and 50 μl of BMP-2 solutions (at concentrations of 0.02, 0.04, 0.1, 0.2, 1, and 2 $\mu\text{g}/\mu\text{l}$), were carefully injected separately at the same time into the back subcutis of rats. At 1, 2, 3, 4 weeks post-treatment, the rats were sacrificed ($n=6$ for each time point) by an overdose injection of anesthetic and the skin including the injected site ($2 \times 2 \text{ cm}^2$) was carefully removed for the subsequent biological examinations.

3.1. Assessment of bone formation induced by BMP-2 released from self-assembled PA nanofibers

Bone formation was assessed by Dual Energy X-ray Absorptometry (DEXA), biochemical evaluation, and histological analysis.

The bone mineral density (BMD) of new bone formed was measured by DEXA utilizing a bone mineral analyzer (Dichroma Scan 600, Aloka Co., Tokyo, Japan) at 1, 2, 3, and 4 weeks after injection of PA, BMP-2, and PA with BMP-2 solutions in rats. The instrument was calibrated with a phantom of known mineral content. Each scan was performed at a speed of 20 mm s^{-1} and the scanning length was 1 mm. DEXA measurement was performed for 6 samples per each experimental group and the region of interest (ROI) for each sample was $1 \times 1 \text{ cm}^2$.

The skin tissue surrounding the injection site ($2 \times 2 \text{ cm}^2$) of PA, BMP-2, and PA with BMP-2 solutions was removed for following biochemical assays at 1, 2, 3, and 4 weeks after injection.

To analyze the osteogenic differentiation of ectopic bone, the intra-cellular alkaline phosphatase (ALP) activity and bone osteocalcin (OCN) content were determined. ALP activity was determined by the *p*-nitrophenylphosphate (*p*NPP) hydrolysis method using the ALP Assay Kit (Lot. No. TJ791, Wako Pure Chemical Industries, Ltd., Osaka, Japan). The skin tissue was taken out 1, 2, 3, and 4 weeks later. The tissues obtained were freeze-dried and crushed. The crushed tissue was homogenized in the lysis buffer (0.2% IGEPAL CA-630, 10 mM Tris-HCL, 1 mM MgCl_2 , pH 7.5). The sample lysate (2 ml) was centrifuged at 12,000 rpm for 10 min at 4 $^\circ\text{C}$. The supernatant was assayed for ALP activity, using *p*-nitrophenyl-phosphate as substrate. To each well of 96 well multi-well culture plates (well area = 28.26 mm^2 , Code 3526, Corning Inc., NY, USA), an aliquot (2.5 μl) of supernatant was added to 25 μl of 56 mM 2-amino 2-methyl-1,3-propanediol (pH 9.8) containing 10 ml *p*-nitrophenyl-phosphate with 1 mM MgCl_2 , and the mixture was incubated at 37 $^\circ\text{C}$ for 30 min. Then 250 μl of 0.02 N NaOH was added to the wells to stop the reaction before absorption at 405 nm was measured with a spectrophotometer. ALP was determined as millimoles of *p*-nitrophenyl released per scaffold after 30 min incubation. To determine the osteocalcin content, the crushed tissue was treated with 1 ml of 40% formic acid for 10 days at 4 $^\circ\text{C}$ under vortex mixing to decalcify. After the decalcification process, the cell extraction was applied to a SephadexTM G-25 column (PD-10, Amersham Pharmacia Biotech, Sweden) for gel filtration. The resulting solution was freeze-dried and subjected to an osteocalcin rat enzyme-linked immunosorbent assay (ELISA) (rat osteocalcin ELISA system, Amersham Bioscience, Tokyo, Japan).

For histological analysis, once they were removed from the subcutaneous sites on the back of rats, the tissues were fixed in 10 wt.% neutral buffered formalin solution, dehydrated in sequentially increasing ethanol solutions to 100 vol.% ethanol, immersed in xylene, and embedded in paraffin. The skin tissues were cross-sectioned to 5 μm thickness with a Tissue-Tek (OCT compound, Miles Inc., USA) and stained with Mayer's hematoxylin–eosin (H–E) solution. These specimens were observed on Olympus AX-80 fluorescence microscope equipped with Olympus DP50 digital camera (KS Olympus, Tokyo, Japan).

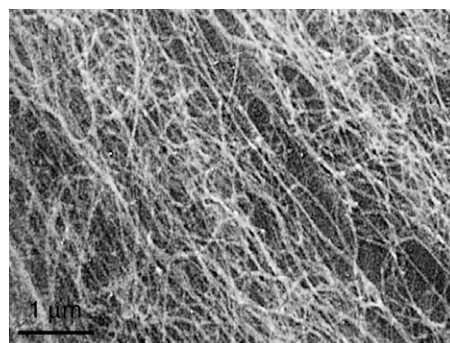


Fig. 1. SEM photograph of self-assembled PA nanofibers network. The concentration of BMP-2 is 0.2 $\mu\text{g}/\mu\text{l}$.

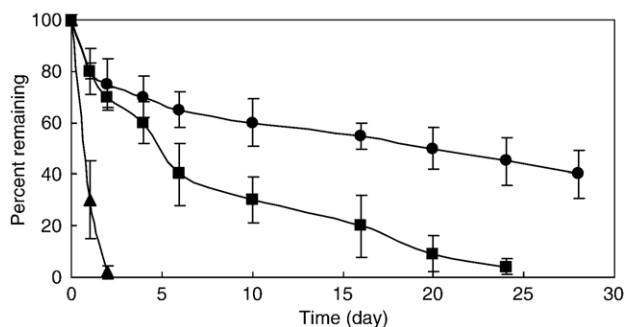


Fig. 2. Time course of radioactivity remaining of ^{125}I -labeled PA and ^{125}I -labeled BMP-2 after subcutaneous injection of free ^{125}I -labeled BMP-2 (▲), self-assembled PA nanofibers incorporating ^{125}I -labeled BMP-2 (■), and self-assembled ^{125}I -labeled PA nanofibers incorporating BMP-2 (●) into the back subcutis of rat. $n=6$, number of rats used for each time point.

3.2. Statistical analysis

All the data were statistically analyzed to express the mean \pm the standard deviation (SD) of the mean. Student's t test was performed and $p < 0.05$ was accepted to be statistically significant.

4. Results

4.1. Morphology of self-assembled PA nanofibers

Fig. 1 shows SEM photograph of nanofibers formed through self-assembly of PA. SEM photograph of self-assembled PA revealed the formation of fibrous assemblies of nanofibers with an extremely high aspect ratio, and high surface areas.

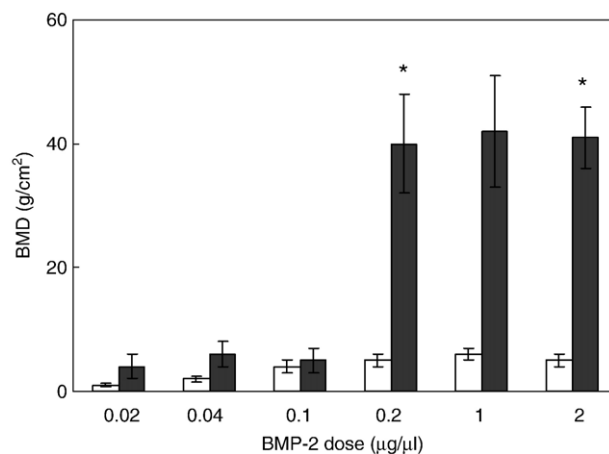


Fig. 4. Effect of BMP-2 dose on the bone mineral density (BMD) of tissues around the injected site of rats 4 weeks after subcutaneous injection of free BMP-2 (□) and BMP-2 with PA (■). *, $p < 0.05$; significant. $n=6$, number of rats for each group.

4.2. In vivo degradation of self-assembled PA nanofibers and in vivo release profile of BMP-2

Fig. 2 shows the time course of self-assembled PA nanofibers and BMP-2 radioactivity remaining after subcutaneous injection of ^{125}I -labeled PA with BMP-2 and PA with ^{125}I -labeled BMP-2. The remaining radioactivity of PA decreased with time, although the degradation time was slow and the PA was retained in the body over 28 days. On the other hand, the residual radioactivity of BMP-2 steeply decreased within 1 day of injection, but thereafter gradually decreased with time. The

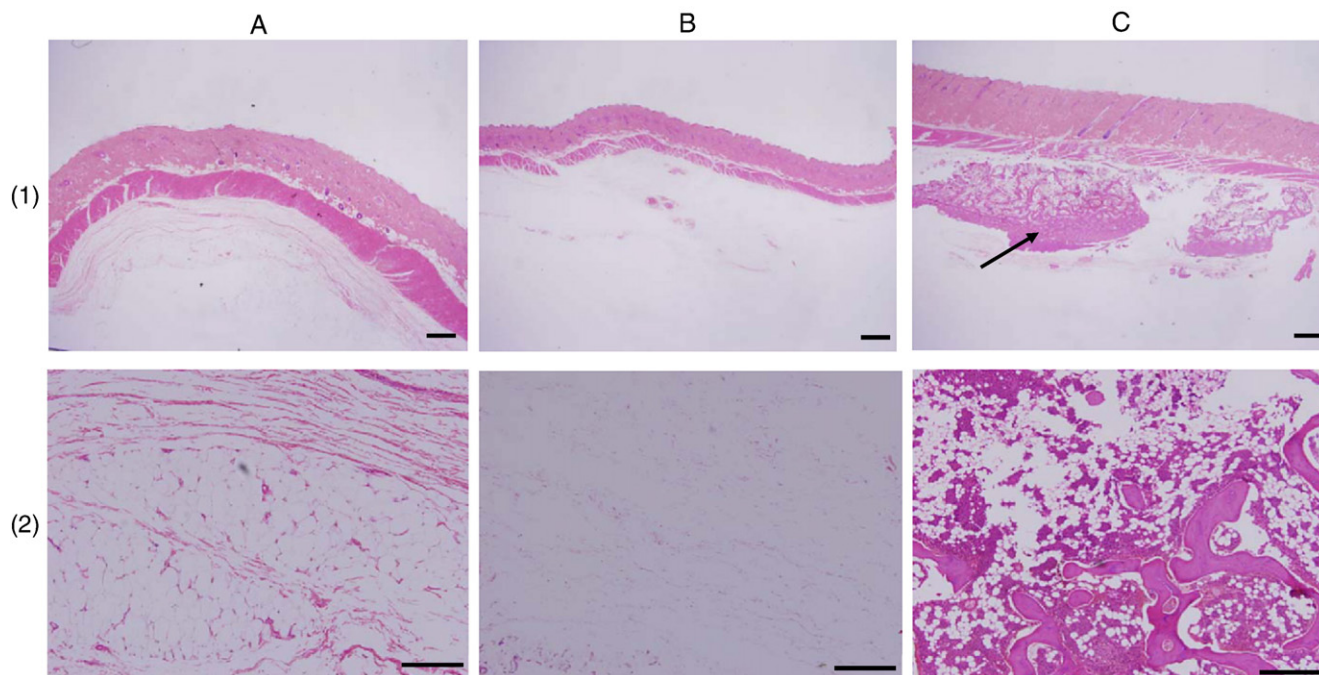


Fig. 3. Histological cross-sections of ectopically formed bone 4 weeks after subcutaneous injection of PA (A), BMP-2 (B), and BMP-2 with PA (C). The concentration of BMP-2 is $0.2 \mu\text{g}/\mu\text{l}$. Each specimen subjected to H-E staining. Arrow indicates the newly formed bone. The scale bar measures 1 mm in full cross-section (1) and $100 \mu\text{m}$ in higher magnification views of center of the sample (2).

radioactivity following injection of only ^{125}I -labeled BMP-2 disappeared within 2 days.

4.3. Ectopic bone formation induced by BMP-2 released from self-assembled PA nanofibers

The BMD of newly ectopic bone formation was significantly enhanced after subcutaneous injection of PA and BMP-2 solution. On the contrary, the injection of BMP-2 alone did not exhibit BMD and the level was as the same as rats after subcutaneous injection of PBS or PA. The BMD values ranged from $34.2 \pm 4.2 \text{ g/cm}^2$ (after 3 weeks) and $44.3 \pm 1.2 \text{ g/cm}^2$ (after 4 weeks), after subcutaneous injection of PA and BMP-2. No significant difference in the BMD was observed between experimental groups.

Fig. 3 shows histological sections of rat subcutis 4 weeks after subcutaneous injection of PA solution, free BMP-2, and BMP-2 injection with PA. A transparent gel was formed only after injection of BMP-2 with PA. The injection of PA alone did not contribute in the formation of gel (data are not shown). Histological analysis revealed that when BMP-2 was injected together with PA solution, the new bone was homogeneously formed at the injected site.

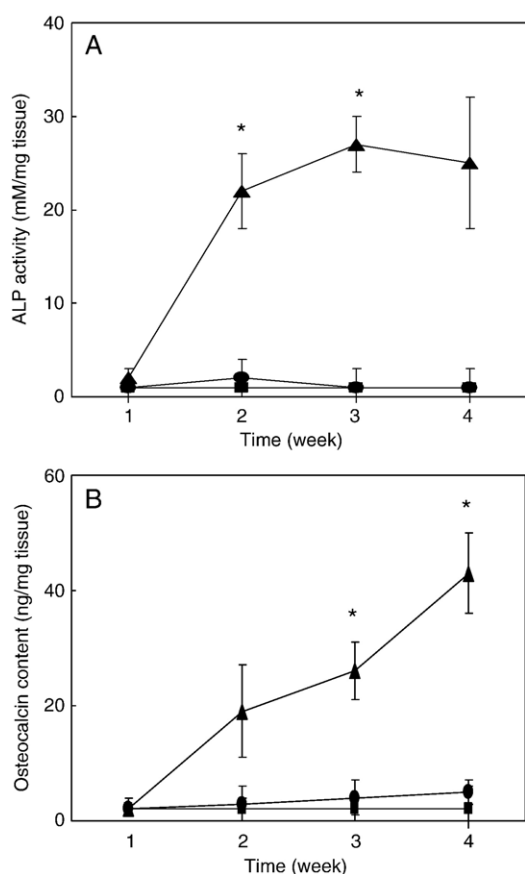


Fig. 5. Time course of ALP activity (A) and osteocalcin contents (B) of tissues around the injected site after injection of PA (■), BMP-2 (●), and BMP-2 with PA (▲). The concentration of BMP-2 is $0.2 \mu\text{g}/\mu\text{l}$. *, $p < 0.05$; significant against the ALP activity (A) or osteocalcin contents (B) of BMP-2 at the corresponding week. $n = 6$, number of rats for each time point.

Fig. 4 shows the effect of the BMP-2 dose on the bone formation (BMD level) induced by self-assembled PA nanofibers. BMP-2-incorporating the self-assembled PA nanofibers significantly enhanced the BMD of new bone formed when the BMP-2 dose was $0.2 \mu\text{g}/\mu\text{l}$ or higher. On the contrary, the injection of BMP-2 alone did not exhibit any significant bone regeneration and the level was as the same as rats treated with PBS and PA (data are not shown).

The ALP activity and osteocalcin content of subcutaneous tissues around the injected site 1, 2, 3, and 4 weeks after subcutaneous injection of PA solution, free BMP-2, and BMP-2 injection with PA are shown in Fig. 5. Significantly higher ALP activity was detected only in the PA-BMP-2 group, where the expression of alkaline phosphatase remained higher than the two other groups 3 weeks after injection. Although it dropped considerably by 4 weeks, the absolute value was not too low, and still higher than in the other groups. After injection, the bone osteocalcin content continued increasing with time only for the PA-BMP-2 group. The OCN content of the skin tissue in the PA-BMP-2 group was much higher than that of the other group at both 3 and 4 weeks after subcutaneous injection.

5. Discussion

The present study demonstrates that the *in vivo* osteoinductive activity of BMP-2 was greatly influenced by incorporation of BMP-2 into self-assembled PA nanofibers. It is known that many growth factors in the body have short half-life lives. To overcome this limitation, growth factors have been encapsulated within different types of polymeric carriers. A potential limitation of the previously developed systems is that they require surgery for implantation. Here we report the synthesis of PA hydrogel scaffolds that incorporate BMP-2.

Many reports have already indicated that it is conceivable to incorporate the growth factors to a sustained releasing system prior to the implantation [20–22]. It has been shown that one approach towards scaffold design is through biomimetic technology [23]. It has been reported that, the modification of scaffolds with peptide sequences can facilitate cellular functions such as adhesion, proliferation and migration [24].

In vivo degradation rate of self-assembled PA nanofibers and *in vivo* release profiles of BMP-2 were estimated in terms of the radioactivity loss of ^{125}I -labeled PA and ^{125}I -labeled BMP-2. As shown in Fig. 2, the PA slowly degraded in the animal body. The results of *in vivo* release profile indicate that BMP-2 was released from self-assembled PA nanofibers in the body as a result of combination of diffusion and degradation mechanisms. The prolonged release of BMP-2 is continued for 20 days after which approximately 90% of the total loaded protein had been released. However, the type of interaction forces acting between BMP-2 and PA molecules is not clear at present. *In vivo* release profiles of BMP-2 at higher concentrations showed an initial burst release followed by the same pattern of BMP-2 release profile at concentration of $0.2 \mu\text{g}/\mu\text{l}$ (data are not shown).

Fig. 3 clearly indicates that subcutaneous injection of BMP-2 together with PA was effective in enhancing BMP-2-induced

ectopic bone. Histological examination demonstrated that bone regenerated around the injection site of self-assembled PA nanofibers incorporated BMP-2, in contrast to sites injected with an aqueous solution of BMP-2. In contrast, the direct injection of a saline solution containing BMP-2 or the injection of PA alone was not effective in inducing ectopic bone. These results correlate with the *in vivo* release profile of BMP-2 (Fig. 2). The subcutaneous injection of PA in rats did not result in an inflammatory reaction around the injection site and, therefore, the PA–BMP-2 complex appears to be a potentially useful biomaterial for *in vivo* applications. It was further demonstrated that lower doses of BMP-2-incorporated into self-assembled PA nanofibers were less capable of forming ectopic bone (Fig. 4). BMP-2 at dose of higher than 0.2 $\mu\text{g}/\mu\text{l}$ was effective to significantly enhance bone formation when injected in BMP-2-incorporated self-assembled PA nanofibers. No induction in ectopic bone was observed even when the amount of BMP-2 in solution that was injected was increased to 1 mg per rat (data are not shown). This must be due to a rapid elimination of BMP-2 from the injection site. In contrast, the BMP-2 incorporated in self-assembled PA nanofibers enabled us to reduce the dose that was effective in inducing significant bone formation to 0.2 $\mu\text{g}/\mu\text{l}$. This finding strongly suggests that the BMP-2-incorporated self-assembled PA nanofibers still maintain their biological activity even though exposed to an *in vivo* environment. It is highly possible that the slow degradation of the BMP-2-incorporated self-assembled PA nanofibers achieves a longer period of BMP-2 release, resulting in induction of ectopic bone formation.

Alkaline phosphatase is an ectoenzyme, produced by osteoblasts, that is likely to be involved in the degradation of inorganic pyrophosphate to provide a sufficient local concentration of phosphate or inorganic pyrophosphate for mineralizing bone. Therefore, ALP is a useful marker for osteoblast activity. Osteocalcin (OCN), also known as bone Gla protein, is a highly conserved non-collagenous protein that contains three γ -carboxyglutamic acid residues that allow it to bind calcium. Although the function of OCN is not quite clear, it is well recognized that only osteoblasts or cells with osteoblastic nature produce OCN. OCN is already known to play an important role in the process of ossification for bone formation. Like alkaline phosphatase, osteocalcin is also selected as a marker of osteogenic differentiation. In our study (Fig. 5), the ALP activity increased rapidly and saturated at 3 weeks, while the temporal changes in the OCN content increased steadily with time, which was in good accordance with the course of bone formation in the subcutaneous tissue. BMP-2 incorporated self-assembled PA nanofibers significantly increased both the ALP and OCN levels compared with free BMP-2 injection.

6. Conclusion

The BMP-2 incorporated PA developed in this study was found to be useful for growth factor release. It is highly possible that the slow degradation of the BMP-2-incorporated self-assembled PA nanofibers achieves a longer period of BMP-2 release, resulting in inducing ectopic bone formation. As a flexible delivery system, these scaffolds can be adapted for

sustained release of many different biomolecules. Incorporation of other growth factors such as bFGF and combination with cell seeding into the matrix is currently under investigation. These results strongly suggest that the controlled release of BMP-2 from BMP-2-incorporated self-assembled PA nanofibers play an important role in creating an environment suitable to induce bone regeneration.

Acknowledgments

This study was performed through the Special Coordination Funds for Promoting Science and Technology from the MEXT, Japan, and partially supported by the research promotion bureau (No. 16-794), MEXT, Japan.

References

- [1] H. Yamagiwa, N. Endo, K. Tokunaga, T. Hayami, H. Hatano, H.E. Takahashi, In vivo bone-forming capacity of human bone marrow-derived stromal cells is stimulated by recombinant human bone morphogenetic protein-2, *J. Bone Miner. Metab.* 19 (2001) 20–28.
- [2] H. Ueda, L. Hong, M. Yamamoto, K. Shigeno, M. Inoue, T. Toba, M. Yoshitani, T. Nakamura, Y. Tabata, Y. Shimizu, Use of collagen sponge incorporating transforming growth factor-beta1 to promote bone repair in skull defects in rabbits, *Biomaterials* 23 (2002) 1003–1010.
- [3] H. Nagai, R. Tsukuda, H. Mayahara, Effects of basic fibroblast growth factor (bFGF) on bone formation in growing rats, *Bone* 16 (1995) 367–373.
- [4] E.A. Wang, V. Rosen, J.S. D'Alessandro, M. Bauduy, P. Cordes, T. Harada, D.I. Israel, R.M. Hewick, K.M. Kerns, P. LaPan, Recombinant human bone morphogenetic protein induces bone formation, *Proc. Natl. Acad. Sci. U. S. A.* 87 (1990) 2220–2224.
- [5] A.W. Yasko, J.M. Lane, E.J. Fellingner, V. Rosen, J.M. Wozney, E.A. Wang, The healing of segmental bone defects, induced by recombinant human bone morphogenetic protein (rhBMP-2), *J. Bone Jt. Surg., Am.* 74 (1992) 659–670.
- [6] M. Bostrom, J.M. Lane, E. Tomin, M. Browne, W. Berberian, T. Turek, J. Smith, J. Wozney, T. Schildhauer, Use of bone morphogenetic protein-2 in the rabbit ulnar nonunion model, *Clin. Orthop. Relat. Res.* 327 (1996) 272–282.
- [7] A.H. Reddi, Bone morphogenetic proteins: an unconventional approach to isolation of first mammalian morphogens, *Cytokine Growth Factor Rev.* 8 (1997) 11–20.
- [8] A.H. Reddi, N.S. Cunningham, Initiation and promotion of bone differentiation by bone morphogenetic proteins, *J. Bone Miner. Res. Suppl.* 2 (1993) S499–S502.
- [9] K. Fujimura, K. Bessho, K. Kusumoto, Y. Ogawa, T. Iizuka, Experimental studies on bone inducing activity of composites of atelopeptide type I collagen as a carrier for ectopic osteoinduction by rhBMP-2, *Biochem. Biophys. Res. Commun.* 208 (1995) 316–322.
- [10] K. Kusumoto, K. Bessho, K. Fujimura, J. Akioka, Y. Ogawa, T. Iizuka, Prefabricated muscle flap including bone induced by recombinant human bone morphogenetic protein-2: an experimental study of ectopic osteoinduction in a rat latissimus dorsi muscle flap, *Br. J. Plast. Surg.* 51 (1998) 275–280.
- [11] Y. Okubo, K. Bessho, K. Fujimura, Y. Konishi, K. Kusumoto, Y. Ogawa, T. Iizuka, Osteoinduction by recombinant human bone morphogenetic protein-2 at intramuscular, intermuscular, subcutaneous and intrafatty sites, *Int. J. Oral Maxillofac. Surg.* 29 (2000) 62–66.
- [12] E.C. Downs, N.E. Robertson, T.L. Riss, M.L. Plunkett, Calcium alginate beads a slow-release system for delivering angiogenic molecules *in vivo* and *in vitro*, *J. Cell. Physiol.* 152 (1992) 422–429.
- [13] S. Miyamoto, K. Takaoka, T. Okada, H. Yoshikawa, J. Hashimoto, S. Suzuki, K. Ono, Evaluation of polylactic acid homopolymers as carriers for bone morphogenetic protein, *Clin. Orthop.* 294 (1992) 333–343.

- [14] W.R. Gombotz, S.C. Pankey, L.S. Bouchard, J. Ranchalis, P. Puolakkainen, Controlled release of TGF-beta 1 from a biodegradable matrix for bone regeneration, *J. Biomater. Sci., Polym. Ed.* 5 (1993) 49–63.
- [15] Z. Ma, M. Kotaki, R. Inai, S. Ramakrishna, Potential of nanofiber matrix as tissue-engineering scaffolds, *Tissue Eng.* 11 (2005) 101–116.
- [16] J.D. Hartgerink, E. Beniash, S.I. Stupp, Self-assembly and mineralization of peptide–amphiphile nanofibers, *Science* 294 (2001) 1684–1688.
- [17] G.B. Fields, R.L. Noble, Solid phase peptide synthesis utilizing 9-fluorenylmethoxycarbonyl amino acids, *Int. J. Pept. Protein Res.* 35 (1990) 161–214.
- [18] M. Ozeki, T. Ishi, Y. Hirano, Y. Tabata, Controlled release of hepatocyte growth factor from gelatin hydrogels based on hydrogel degradation, *J. Drug Target.* 9 (2001) 461–471.
- [19] F.C. Greenwood, W.M. Hunter, T.C. Glover, The preparation of ¹³¹I-labeled human growth hormone of high specific radioactivity, *Biochem. J.* 89 (1963) 114–123.
- [20] A.K. Dogan, M. Gumusderelioglu, E. Aksoz, Controlled release of EGF and bFGF from dextran hydrogels in vitro and in vivo, *J. Biomed. Mater. Res. B Appl. Biomater.* 74 (2005) 504–510.
- [21] A. Iwakura, Y. Tabata, N. Tamura, K. Doi, K. Nishimura, T. Nakamura, Y. Shimizu, M. Fujita, M. Komeda, Gelatin sheets incorporating basic fibroblast growth factor enhances healing of devascularized sternum in diabetic rats, *Circulation* 104 (Suppl 1) (2001) 1325–1329.
- [22] S. Cai, Y. Liu, X.Z. Shu, G.D. Prestwich, Injectable glycosaminoglycan hydrogels for controlled release of human basic fibroblast growth factor, *Biomaterials* 26 (2005) 6054–6067.
- [23] K.M. Woo, V.J. Chen, P.X. Ma, Nano-fibrous scaffolding architecture selectively enhances protein absorption contribution to cell attachment, *J. Biomed. Mater. Res. A* 67 (2003) 531–537.
- [24] H. Shin, S. Jo, A.G. Mikos, Biomimetic materials for tissue engineering, *Biomaterials* 24 (2003) 4353–4364.